ELSEVIER

Journal of Nuclear Materials 288 (2001) 222–232

journal of nuclear materials

www.elsevier.nl/locate/jnucmat

Letter to the Editors

Microstructure and mechanical properties of Inconel 625 superalloy

Vani Shankar, K. Bhanu Sankara Rao *, S.L. Mannan

Materials Development Group, Indira Gandhi Center for Atomic Research, Kalpakkam 603102, India

Received 7 July 2000; accepted 21 November 2000

Abstract

The service-exposed (~60 000 h/873 K) Alloy 625 ammonia cracker tubes showed higher strength and lower ductility compared to the virgin material in the solution annealed state. Precipitation of intermetallic γ'' and $Ni_2(Cr,Mo)$ phases and the inter and intragranular carbides were found to be responsible for higher strength of the service-exposed alloy. Subjecting the service-exposed alloy to thermal aging treatments subsequently at 923 K and 1123 K (above the service temperature of the exposed alloy) led to the dissolution of the intermetallic phases that in turn increased the ductility of the alloy. Post-service aging of the alloy at 923 K for short durations resulted in the dissolution of the $Ni_2(Cr,Mo)$-phase. The dissolution of the $Ni_2(Cr,Mo)$-phase exhibited significant influence upon yield strength (YS) but negligible effect on ductility. Prolonged aging of the alloy for 500 h at 923 K resulted in the precipitation of intermetallic δ-phase. Post-service aging of the alloy at 1123 K promoted the dissolution of both $Ni_2(Cr,Mo)$ and γ'' formed during service. Longer duration aging at the same temperature led to the precipitation of the δ-phase with an associated increase in strength and loss in ductility. Re-solution annealing of the service-exposed alloy at 1423 K caused the dissolution of the strengthening phases. When the re-solution annealed alloy was subjected to prolonged exposure at 923 K, the yield stress was found to increase rapidly with aging time with attendent loss in ductility due to the precipitation of γ''.

1. Introduction

Inconel 625 (Alloy 625) is a wrought nickel-based superalloy strengthened mainly by the additions of carbon, chromium, molybdenum, and niobium. Developed for service at temperatures below 973 K, this alloy combines the high strength of the age-hardening nickel-based alloys with excellent fabrication characteristics. Apart from its widespread applications in aeronautic, aerospace, marine, chemical and petrochemical industries, it is also being used for reactor-core and control-rod components in pressurized water reactors and as heat exchanger tubes in ammonia cracker plants for heavy water production. Excellent corrosion behavior in cracked ammonia environments and outstanding creep resistance are the major features responsible for the importance of this alloy in heavy water plants. Although the alloy was initially designed as a solid solution hardened alloy, it has been observed that precipitation of intermetallic phases and carbides occur on subjecting the alloy to aging treatment in the range 823–1023 K [1]. Precipitation hardening in this alloy at elevated temperatures (823–923 K) is mainly derived from the metastable phase γ'' [$Ni_3(Nb,Al,Ti)$] having ordered body-centered tetragonal DO_{22} structure [2]. The metastable γ''-phase gets transformed to the orthorhombic δ-phase [$Ni_3(Nb,Mo)$] upon prolonged aging [2–7]. The δ-phase has also been reported to form directly from the supersaturated solid solution on aging at temperatures higher than 1023 K [8]. Precipitation of $M_{23}C_6$, M_6C and MC carbides will occur in the range 1033–1253 K [9]. The primary MC carbides present in the undissolved state during solution annealing have been reported to decompose into $M_{23}C_6$ and M_6C on prolonged exposure at elevated temperatures [9].

* Corresponding author. Tel.: +91-4114 40 232; fax: +91-4114 40 360.

E-mail address: bhanu@igcar.ernet.in (K. Bhanu Sankara Rao).

0022-3115/01/$ - see front matter
PII: S0022-3115(00)00723-6

The effect of the above transformations on mechanical properties have not been examined in detail though few attempts have been made earlier to characterize the evolving microstructure upon prolonged exposure [10–16]. Recent investigations have revealed precipitation of $Ni_2(Cr,Mo)$-phase in Alloy 625, which has Pt_2 Mo-type structure by prolonged aging at temperatures below 873 K [10]. Presence of this orthorhombic phase has been credited with low tensile and creep ductility and toughness in superalloys [10,13,14,17]. In this paper, we shall describe the microstructural features observed in Alloy 625 after different heat treatments and also the room temperature tensile properties determined after these treatments. The heat treatment conditions examined include: (i) service exposure at 873 K for ~60 000 h, (ii) aging the service-exposed alloy at temperatures higher than service temperatures for different durations, (iii) re-solution annealing and aging at different temperatures. This paper correlates the mechanical behavior with the microstructural changes occurring with various heat treatments.

2. Experimental

The current investigation has been conducted on Alloy 625 tube retrieved from an ammonia cracker plant after 60 000 h of service at approximately 873 K. The tube had a wall thickness of 9 mm with outer diameter of 90 mm. The blanks of $60 \times 10 \times 9$ mm^3 were cut from the service-exposed tubes in the longitudinal direction and subsequently subjected to various heat treatments listed in Table 1. The nominal chemical composition of the alloy in wt% is as follows: Cr-20 to 30%, Fe-5% max, Mo-8 to 10%, (Nb + Ta)-3.15–4.15%, C-0.1%, Mn-0.5%, Si-0.5%, P-0.015%, S-0.015%, Al-0.40%, Ti-0.4%, Co-1% and Ni-balance.

Specimens for optical microscopy (OM) and scanning electron microscopy (SEM) were taken from the service-exposed as well as heat-treated blanks. The samples for OM were prepared by mechanical polishing followed by electrochemical etching. Electrolytic etching was carried out in saturated oxalic acid solution at ~3–5 V using a stainless steel cathode for nearly 20 s.

Specimens for transmission electron microscopy (TEM) were prepared from 1 mm slices taken from the blanks. The slices were first ground mechanically to a thickness of about 0.10–0.15 mm. Discs were subsequently punched from these ground samples and were thinned by the dual jet electro polishing technique. Electro polishing was carried out at ~20 V in a medium containing one part of perchloric acid and four parts of ethanol. Temperature of the bath was maintained at ~230 K during electro polishing.

Tensile test specimens of 4 mm diameter and 25 mm gauge length were machined from the service-exposed as well as from the samples subjected to various heat treatments. Tensile tests were conducted at room temperature in air using a floor model 1195 Instron Universal testing machine. A constant strain rate of 3.3×10^{-4} s^{-1} was employed for all the tests.

3. Results and discussion

3.1. Microstructure

3.1.1. Service-exposed condition

Optical microscopy of the polished and lightly etched sample of service-exposed alloy showed continuous thick film of carbides along the grain boundaries and undissolved blocky particles randomly distributed in the intra and intergranular regions (Fig. 1). These relatively coarse particles could be clearly seen as whitish areas in Fig. 1. Electron probe micro analysis (EPMA) of the grain boundary blocky precipitates clearly proved that these particles are rich in niobium and carbon (Fig. 2(a)). It appears that these precipitates nucleated in the melt and were not dissolved during the solution treatment given to the alloy, prior to employing in service. These blocky precipitates will be referred here after as primary niobium carbides. Line scans carried out across the blocky white precipitates revealed the presence of both Nb and Mo (Fig. 2(b)). Few carbides showed absence of Mo in the vicinity of Nb enrichment (Fig. 2(c)). TEM revealed extensive precipitation of fine particles in the intragranular regions and a thick continuous grain boundary layer of carbides (Fig. 3(a)). Magnified image

Table 1
Details of heat treatments employed

S. No.	Condition	Aging treatment temperature (K)	Duration (h)	Remarks
1	Service-exposed	–	–	Exposed to ~873 K for ~60 000 h
2	Post-service Aging treatment	(i) 923 (ii) 1123	1, 100, 200, 500 1, 10, 30, 100, 200, 500	–
3	Re-solution annealed (1423 K) + aging treatment	(i) 923 (ii) 1123	1, 10, 100, 200, 500 1, 10, 100, 200, 500	–

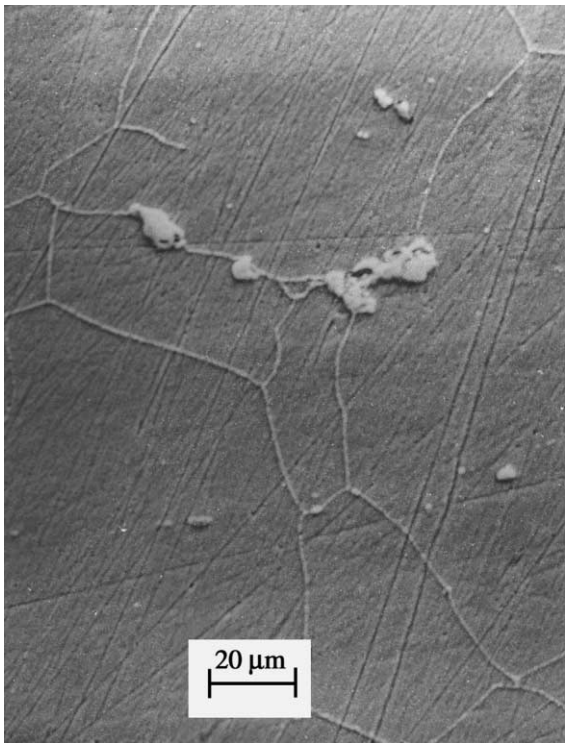

Fig. 1. Optical micrograph showing large primary carbides, continuous film of grain boundary (g.b.) carbides and discrete matrix carbides.

of the insert in Fig. 3(a) showed that the intragranular precipitates were having snow flaky morphology (Fig. 3(b)). Selected area diffraction (SAD) patterns taken from the matrix using [0 0 1] zone axis displayed superlattice reflections at {1 0 0}, {1 1 0}, {1 1/2 0} and 1/3{2 2 0} positions in addition to the matrix reflections (Fig. 3(c)). The {1 0 0}, {1 1 0} and {1 1/2 0} was associated with the elliptical shaped γ'' and the superlattice reflection at 1/3{2 2 0} positions in the SAD belonged to the $Ni_2(Cr,Mo)$-phase that portrayed snow flake-like morphology.

3.1.2. Post-service aging treatment at 923 K

Aging for 1 h at 923 K triggered the dissolution of the $Ni_2(Cr,Mo)$-phase. Discrete carbides at the grain boundaries and evenly distributed elliptical shaped γ'' within the matrix could be observed (Fig. 4). The dark field micrograph, Fig. 4(b), shows clearly the uniform distribution of γ'' precipitates throughout the matrix. The intensity of superlattice reflections (Fig. 4(c)) of γ''-phase is quite large as a result of large differences in the atomic scattering factors of the Ni and Nb atoms constituting the γ''-phase. Subjecting the alloy for 10 h at 923 K caused the complete dissolution of the $Ni_2(Cr,Mo)$-phase. The SAD pattern using [0 0 1] zone axis of the service-exposed alloy

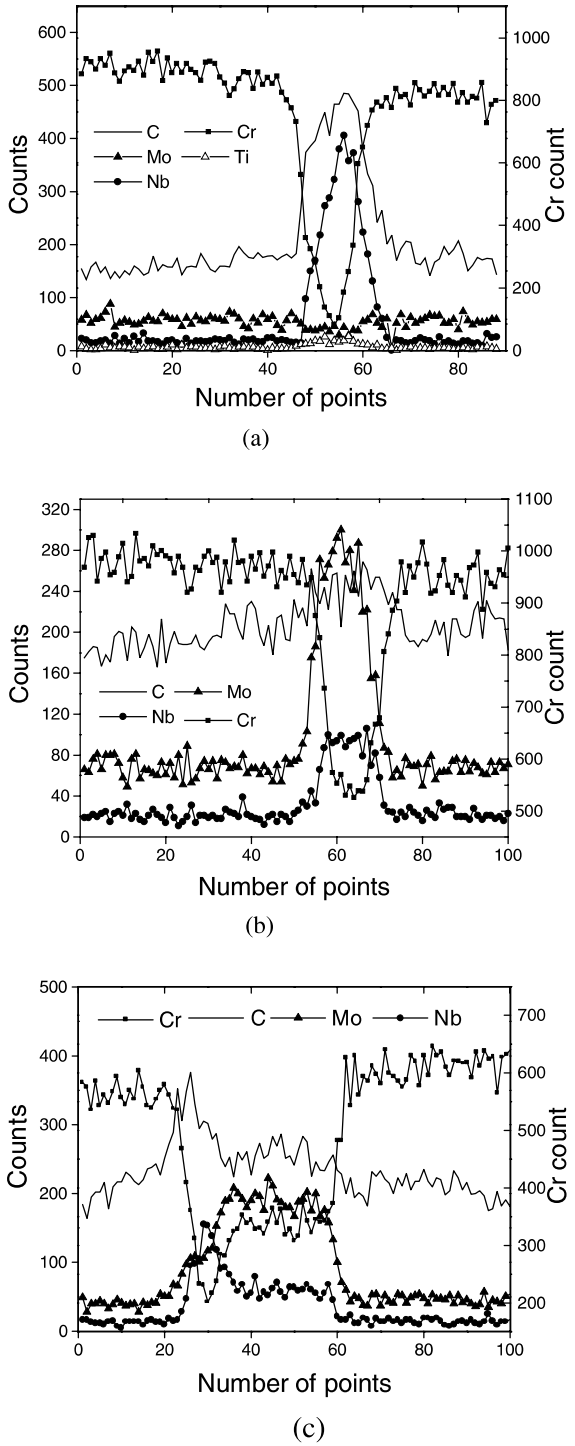

Fig. 2. Line scans of service-exposed alloy taken across: (a) whitish areas in grain boundary regions of Fig. 1 show Nb and C enrichment; (b) matrix carbides show both Nb & Mo enrichment; (c) one of the matrix carbides show Nb and Mo redistribution.

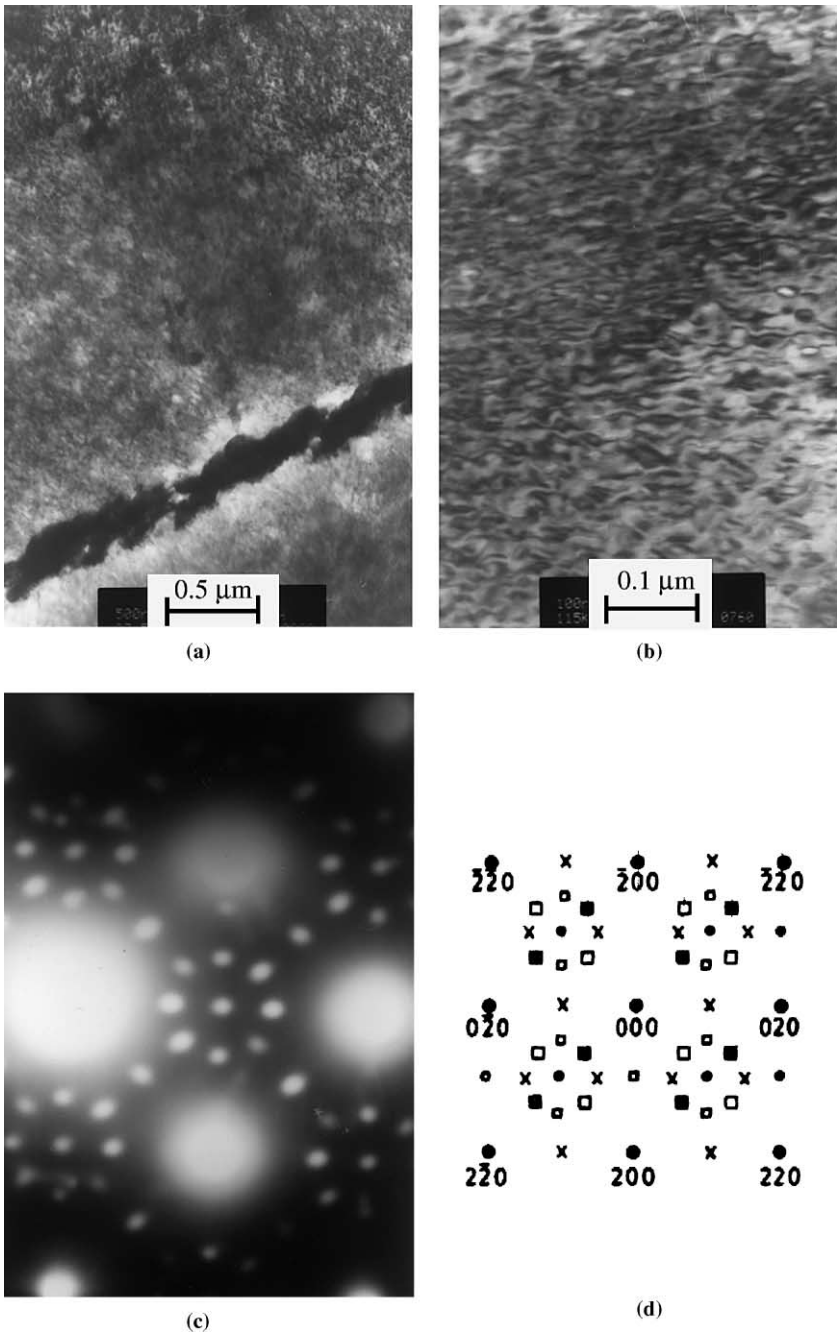

Fig. 3. (a) BF image of service-exposed alloy showing extensive intragranular precipitation and continuous film of carbides on grain boundaries. (b) Magnified image of Fig. 3(a) shows snowflaky morphology of $Ni_2(Cr,Mo)$-phase. (c) SAD taken from matrix using [0 0 1] zone axis shows superlattice reflections of both $Ni_2(Cr,Mo)$ and γ'' precipitates. (d) Key to diffraction pattern shown in (c).

indicated strong reflections corresponding to both $Ni_2(Cr,Mo)$ and γ'' phases along with the γ matrix (Fig. 3(c)) while the service-exposed alloy aged for 10 h at 923 K displayed reflections arising only from the γ''-phase (Fig. 5(b)). These observations suggest that the $Ni_2(Cr,Mo)$-phase has undergone dissolution within 10 h of aging. Aging of the service-exposed alloy up to 500 h, led to the nucleation and growth of δ-phase. SEM of lightly etched sample clearly showed needle shaped δ-phase in the intragranular regions (Fig. 6).

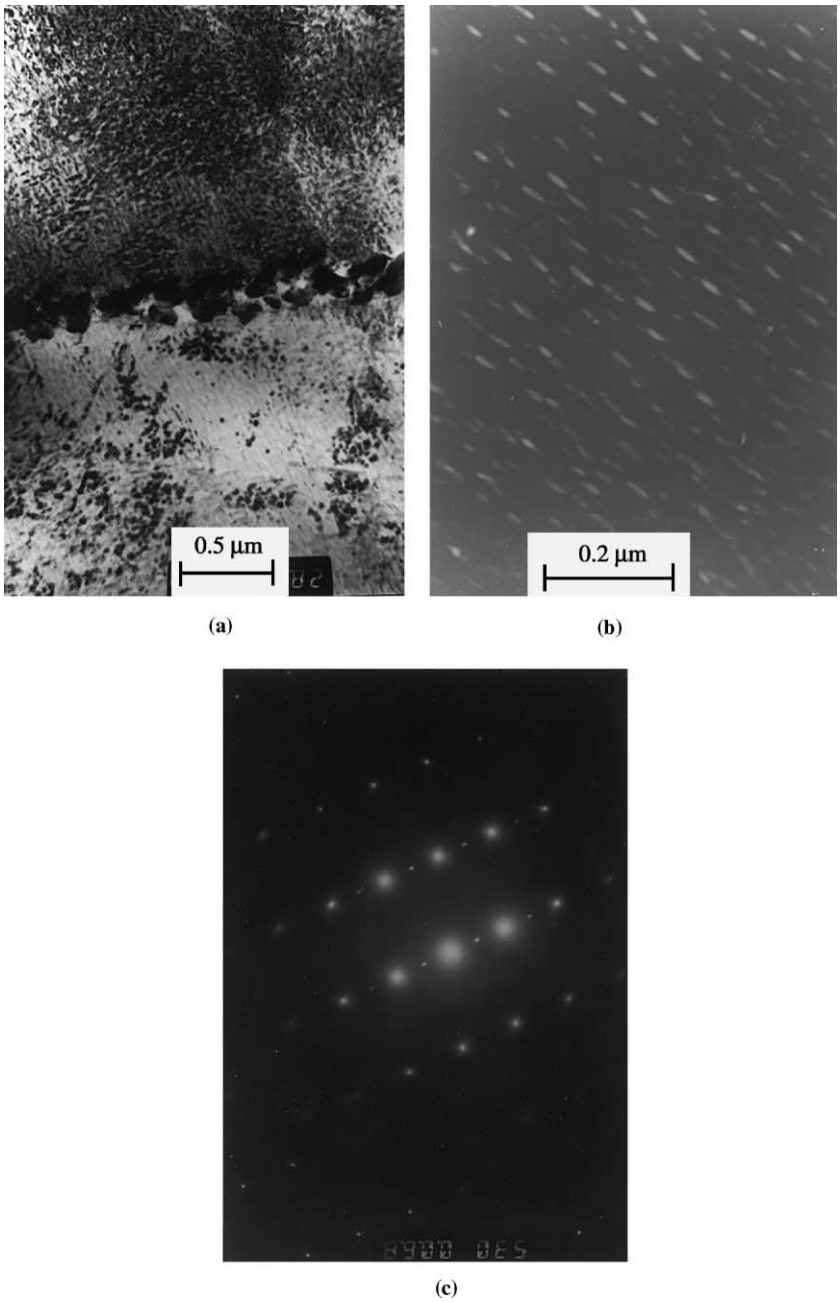

Fig. 4. Service-exposed alloy given 1 h treatment at 923 K: (a) BF taken from matrix shows mainly γ'' and intergranular carbides; (b) DF taken from γ'' reflection shows ellipsoidal γ'' precipitates; (c) SAD taken from matrix shows strong γ'' superlattice reflections.

3.1.3. Post-service aging treatment at 1123 K

Aging the service-exposed alloy at 1123 K for 1 h led to the complete dissolution of the γ'' and $Ni_2(Cr,Mo)$ precipitates. Though the continuous grain boundary carbides were noticed, matrix was found free from any type of precipitation (Fig. 7(a)). Precipitation of δ-phase commenced on aging for durations longer than 1 h. The volume fraction of δ increased with increase in aging period (Fig. 7(b)). It was observed that nucleation of the δ precipitates occurred quite randomly and grew in almost all directions.

3.1.4. Re-solution annealing and aging

Fig. 8 shows a BF image of a service-exposed plus re-solution annealed alloy at 1423 K for 0.5 h. The re-solution annealing caused the dissolution of most of the

(a)

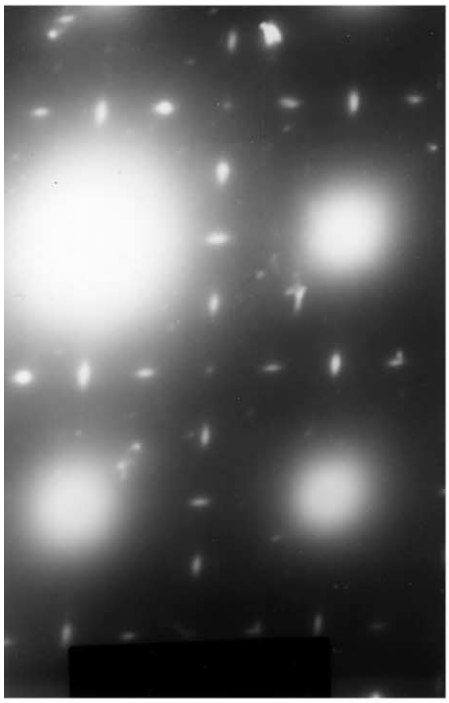

(b)

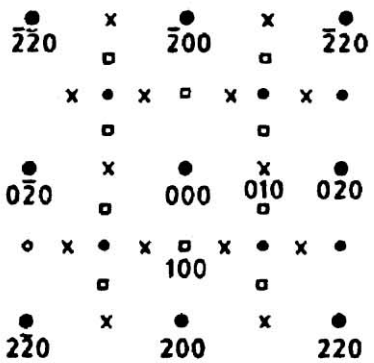

(c)

Fig. 5. Service-exposed material aged at 923 K for 10 h: (a) BF shows intergranular carbides and γ''; (b) SAD taken from matrix using [0 0 1] zone axis shows absence of $Ni_2(Cr,Mo)$ reflections; only matrix and γ'' reflections present; (c) key to diffraction pattern shown in (b).

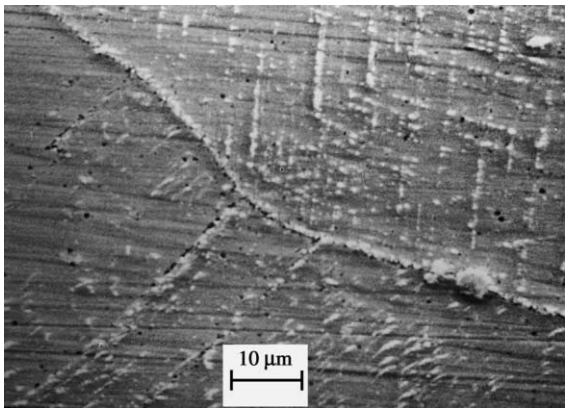

Fig. 6. SEM micrograph of service-exposed sample aged at 923 K for 500 h showing elongated precipitates of δ.

pre-existing precipitates in the service-exposed state. However, a few large primary NbC were found to remain undissolved. The alloy also contained a large number of uniformly distributed dislocations that resulted during quenching operation. Aging the re-solution annealed alloy at 923 K for durations longer than 1 h resulted in the precipitation of γ'' in the matrix and carbide precipitates at grain boundaries (Fig. 9(a)) while aging of the re-solution annealed alloy at 1123 K for 1 h resulted in the precipitation of thin rod shaped δ precipitates. Continued aging caused additional precipitation and coarsening of δ-phase in the intragranular regions (Fig. 9(b)).

3.2. Mechanical properties

3.2.1. Tensile properties of service-exposed plus aged alloy

The room temperature tensile properties of the service-exposed and re-solution annealed samples subjected to long term aging at 923 and 1123 K are presented in Fig. 10. It can be seen that the aging of the service-exposed alloy at 923 K led to a continuous decrease in yield strength (YS) with aging time up to 200 h (Fig. 10(a)). Beyond 200 h, a marginal increase in YS was noticed. On the other hand, the service-exposed alloy showed a rapid increase in ultimate tensile strength (UTS) on aging at 923 K beyond 1 h. Service-exposed alloy showed a minimum in UTS after 1 h aging at 923 K. On aging the service-exposed alloy at 1123 K, drastic reduction in YS was observed initially. Further aging led to a progressive increase in YS up to 100 h. Beyond 100 h, the YS showed an upward trend. In contrast to a drastic reduction in YS observed, the UTS of the service-exposed plus aged alloy exhibited a sharp increase after aging at 1123 K/1 h (Fig. 10(b)). Prolonged aging at 1123 K caused a decrease in UTS with aging time (Fig. 10(b)). The total elongation of the service-exposed alloy increased steadily with increasing aging time at 923 K up

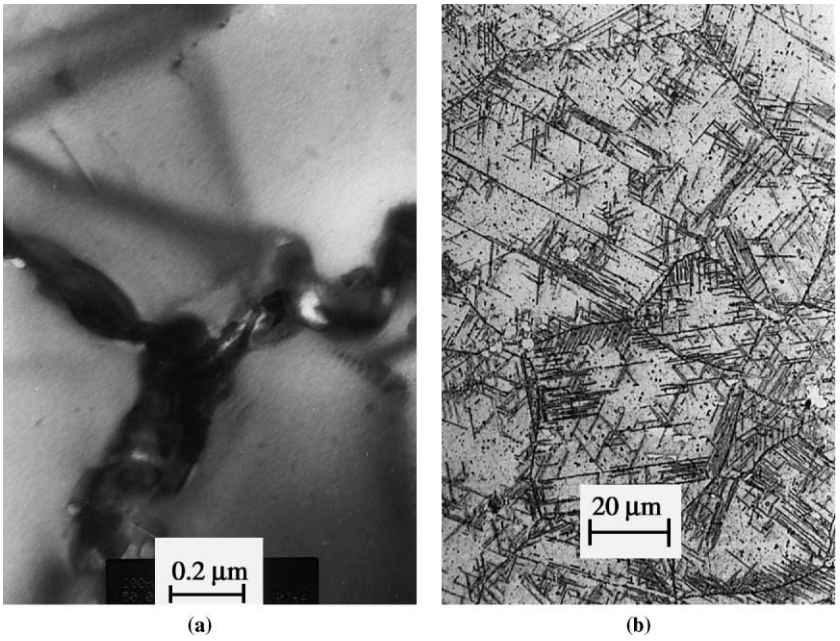

Fig. 7. Service-exposed material aged at 1123 K: (a) for 1 h shows intergranular carbides and absence of $Ni_2(Cr,Mo)$ and γ'' phases; (b) precipitation of δ-phase at the end of 100 h thermal aging.

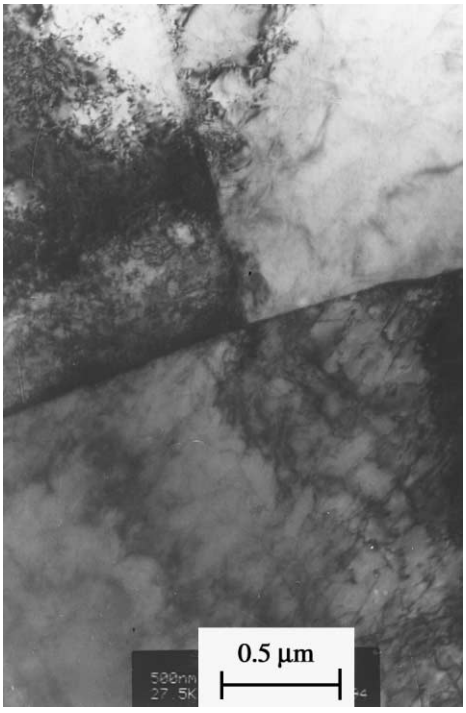

Fig. 8. Service-exposed alloy re-solution annealed at 1423 K for 0.5 h showed clean matrix and g.b.

to 200 h (Fig. 10(c)). A slight reduction was noticed beyond 200 h. Aging at 1123 K showed a peak in total elongation at 1 h (Fig. 10(c)).

3.2.2. Tensile properties of re-solution annealed plus aged alloy

When the re-solution annealed alloy was subjected to aging at 923 K, YS was increased rapidly with aging time while a marginal increase in YS occurred on aging at 1123 K. In general, the UTS of re-solution annealed alloy displayed a sharp increase on aging at 923 K, while aging at 1123 K led to a drastic reduction with increasing duration of aging. The total elongation of re-solution annealed alloy decreased rapidly with time on aging at both the temperatures.

3.3. Correlation of microstructure with mechanical properties

It was observed that the service-exposed material had high YS of ~1013 MPa and a ductility (% elongation to fracture) of ~6% compared to the YS value of 375 MPa and 60% ductility obtained on the virgin material prior to service exposure. The high YS value of the service-exposed alloy is mainly derived from the presence of the strengthening phases γ'' and $Ni_2(Cr,Mo)$ in the matrix. When the service-exposed material was re-solution annealed at 1423 K for 0.5 h and tensile tested at room temperature, it was noticed to have properties very close to the values obtained for the alloy prior to service exposure. This indicates that all the precipitates that were responsible for the strengthening of the alloy underwent dissolution during the re-solution annealing treatment. The sharp decrease in the YS value of the service-exposed alloy upon aging at 1123 K for 1 h is attributed

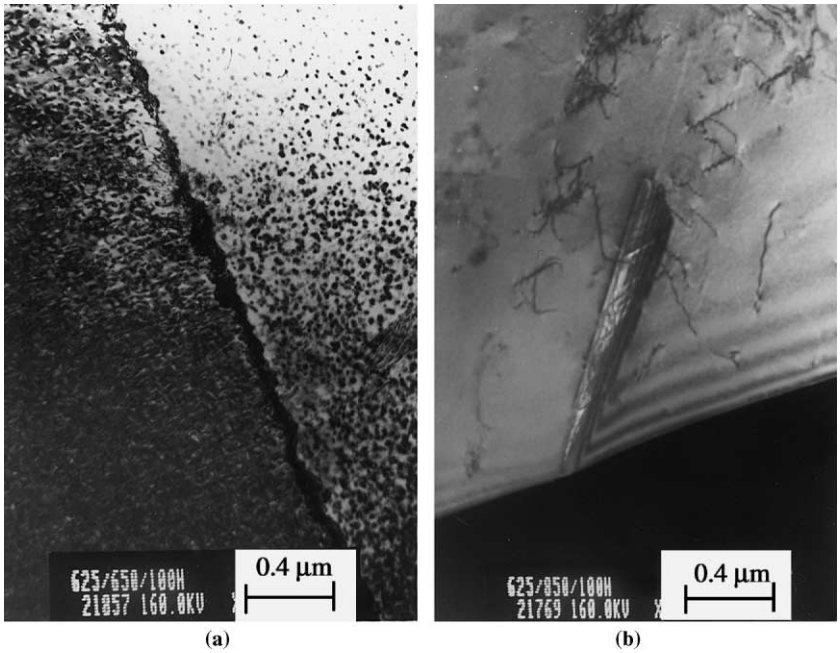

Fig. 9. Re-solution annealed alloy aged at: (a) 923 K for 100 h shows g.b. carbides and γ''; (b) at 1123 K for 100 h shows δ precipitates.

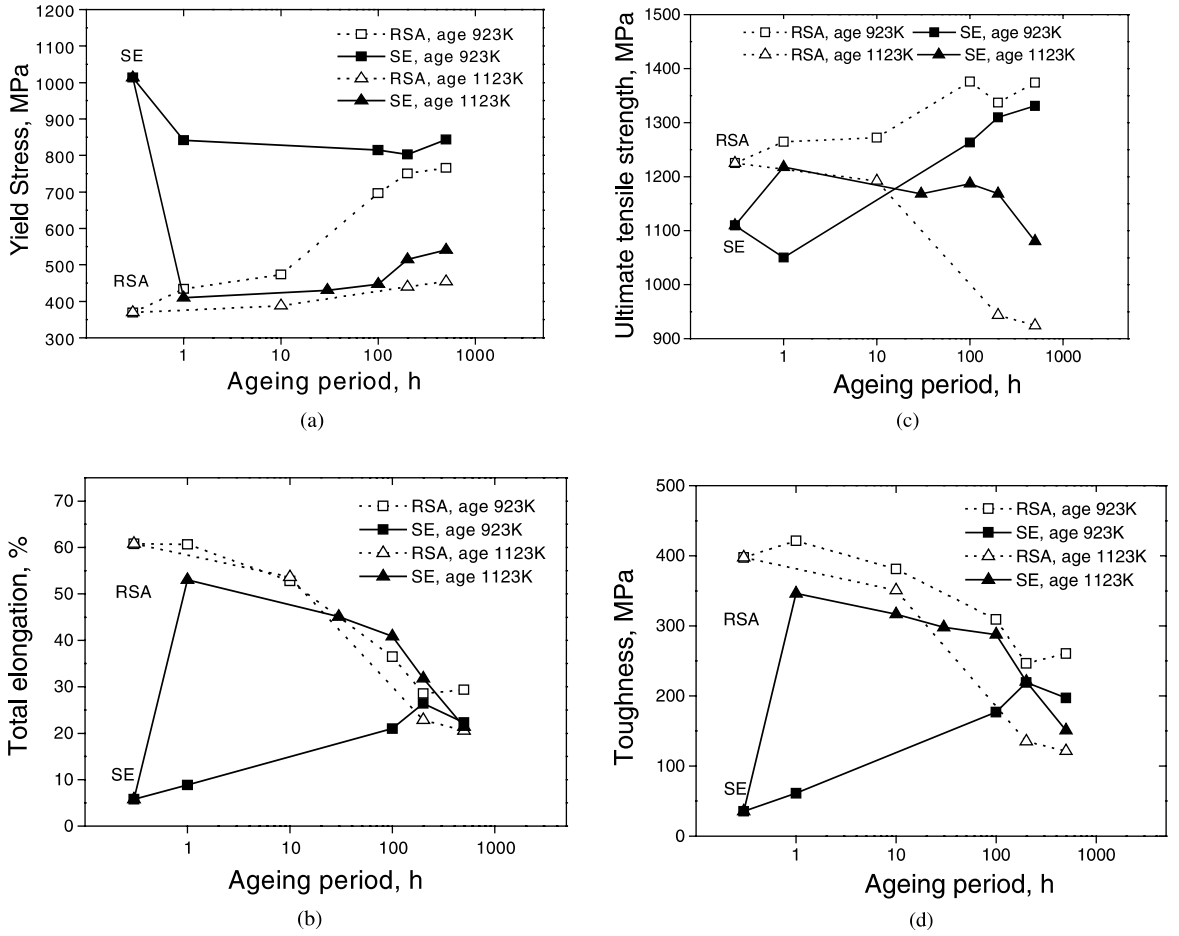

Fig. 10. Variation of: (a) YS; (b) total elongation of service-exposed and re-solution annealed alloy with thermal aging period; (c) ultimate tensile strength; (d) approximate toughness calculated from area under stress–strain curve with aging time.

to the dissolution of the intermetallic phases γ'' and $Ni_2(Cr,Mo)$ (Table 2). Aging beyond 1 h at 1123 K caused a continuous increase in the YS values with a corresponding decrease in the ductility (Fig. 10(a) and (c)). These changes resulted from the precipitation of the δ-phase. The re-solution annealed alloy when aged at the same temperature showed a continuous increase in the YS value and a decrease in ductility right from the beginning (Fig. 10(a) and (c)). However, there was a detectable amount of difference in the YS values for the two conditions upon aging beyond 100 h (Fig. 10(a)). The re-solution annealed material exhibited gradual increase in the YS value over the period of 500 h while the service-exposed alloy showed a very sharp increase in the YS value beyond 100 h. The sharp increase in the YS of the service-exposed alloy is associated with the enhanced precipitation of the δ-phase [$Ni_3(Nb,Mo)$] that occur due to the presence of Mo and Nb rich (Fig. 2) carbides. There was a gradual decrease in the YS value upon aging the service-exposed alloy at 923 K compared to the drastic reduction observed for 1123 K treatment. Also, the YS value for 923 K treatments never reached the YS value of 1123 K-1 h treatment even upon prolonged aging. This observation clearly indicates that the intermetallic phases that go into solution during 1123 K-1 h treatment do not get dissolved at 923 K even after prolonged aging.

The intermetallic orthorhombic δ [$Ni_3(Nb,Mo)$]-phase can form directly from the supersaturated solid solution on aging at relatively high temperatures [8]. Precipitation of δ-phase in Inconel 625 was reported to be very rapid at temperature above 1073 K [6]. Upon aging the re-solution annealed alloy at 1123 K, δ precipitation was observed; the volume fraction has been noticed to increase with increase in aging time. Since the service-exposed alloy was also aged at the same temperature, it showed similar precipitation behavior once all the intermetallic precipitates were dissolved within 1 h of aging treatment at 1123 K (see Table 3). The rapid increase in the YS of the service-exposed alloy beyond

Table 2
Tensile properties of service-exposed (SE) and aged Alloy 625

Heat treatment condition	YS (MPa)	UTS (MPa)	Total elongation (%)
SE	1013	1110	5.8
SE + 923 K; 1 h	842	1050	8.8
SE + 923 K; 100 h	815	1263	21.0
SE + 923 K; 200 h	803	1310	26.4
SE + 923 K; 500 h	844	1331	22.3
SE + 1123 K; 1 h	410	1218	53
SE + 1123 K; 10 h	426	1171	48.3
SE + 1123 K; 30 h	431	1168	45.1
SE + 1123 K; 100 h	447	1187	40.8
SE + 1123 K; 200 h	515	1169	31.8
SE + 1123 K; 500 h	541	1081	21.4
Virgin material (pre-service condition)	375	1225	60.8

Table 3
Tensile properties of re-solution annealed (RSA) plus aged Alloy 625

Heat treatment condition	YS (MPa)	UTS (MPa)	Total elongation (%)
RSA	370	1225	60.8
RSA + 923 K; 1 h	434	1265	60.7
RSA + 923 K; 10 h	473	1272	52.8
RSA + 923 K; 100 h	696	1376	36.5
RSA + 923 K; 200 h	750	1337	28.5
RSA + 923 K; 500 h	766	1374	29.4
RSA + 1123 K; 10 h	388	1192	53.6
RSA + 1123 K; 200 h	440	943	22.8
RSA + 1123 K; 500 h	454	925	20.6

100 h of aging at 1123 K (Fig. 10(a)) can be attributed to the enhanced precipitation of the δ-phase. It was observed that the precipitation of the δ-phase had initiated at the Nb and Mo enriched regions of grain boundary and matrix carbides. Hence it is quite possible that these enriched regions would promote early precipitation of the δ-phase that was responsible for the rapid increase in the YS.

The behavior of the service-exposed alloy upon aging at 923 K was different from the behavior shown by the alloy upon aging at 1123 K. The continuous decrease in the YS and a corresponding increase in ductility up to 200 h were due to the dissolution of the hardening phase. However, aging beyond 200 h caused replacement of γ''-phase with the elongated δ-phase (Fig. 6). It has been observed that the nickel and nickel–iron based superalloys that are precipitation strengthened by the γ''-phase, are susceptible to δ-phase formation [9]. Another striking feature to be noticed in Fig. 10(a) is that there was a large decrease in the YS and a marginal increase in the ductility of the service-exposed alloy upon aging at 923 K for 1 h. Electron microscopy investigations conducted on service-exposed samples aged for short durations at the same temperature had shown dissolution of

Table 4
Details of the tensile property results obtained and their interpretation[a]

S. No.	Condition	Mechanical properties	Interpretation
1.	SE	Poor ductility (~6%); high YS value	Precipitation of intermetallic phases $Ni_2(Cr,Mo)$ and γ'', continuous grain boundary carbide films
2.	SE + 923 K-1 h	Large ↓ YS; slight ↑ ductility	Dissolution of $Ni_2(Cr,Mo)$ prominent
3.	SE + 923 K-500 h	↑ YS; ↓ ductility	Precipitation of δ
4.	SE + 1123 K-1 h	↓ YS; ↓ ductility	Dissolution of $Ni_2(Cr,Mo)$ and γ''
5.	SE + 1123 K-longer aging	↑ YS; large ↓ ductility	Precipitation of δ
6.	SE + 1423 K-0.5 h	↓ YS; ↑ ductility	Dissolution of all $Ni_2(Cr,Mo)$, γ'' and secondary carbides present initially

[a] SE – service-exposed; ↑ increase; ↓ decrease.

$Ni_2(Cr,Mo)$-phase (see Table 4). Thus, the dissolution of $Ni_2(Cr,Mo)$-phase has a large influence upon the YS and only marginal effect on ductility. Strengthening due to precipitation of $Ni_2(Cr,Mo)$-phase and almost non-perceptible change in ductility was reported in case of Hastelloy alloys [13,14]. Strengthening in these alloys has been attributed to the long range ordering reaction whereby the disordered fcc lattice is transformed to orthorhombic Pt_2Mo type superlattice. Detailed investigations by Tawancy [18] has revealed that the deformation in the ordered state occurs by twinning rather than by slip which usually requires greater stress. However, the UTS showed a large increase on aging at 923 K/1 h. This is attributed to the enhanced work hardening associated with γ'' coarsening.

4. Conclusions

1. Sharp decrease in the YS value of the service-exposed material on aging for 1 h at 1123 K resulted from the complete dissolution of the intermetallic phases $Ni_2(Cr,Mo)$ and γ''. Further aging at 1123 K resulted in the precipitation of the δ-phase, with an associated increase in strength. Re-solution annealed alloy also showed precipitation of δ-phase on aging at 1123 K. Precipitation of δ-phase led to low ductility values.

2. Aging of re-solution annealed alloy at 923 K caused improvement in YS and reduction in ductility with aging time. The increased strength resulted from precipitation of γ''-phase. The $Ni_2(Cr,Mo)$-phase precipitated during service has been dissolved completely on subjecting the alloy for 10 h exposure at 923 K. Its dissolution has more influence upon the YS of the alloy than on ductility. Longer aging of the service-exposed alloy at 923 K promoted coarsening of the γ'' precipitates. Prolonged aging of the service-exposed alloy at 923 K also resulted in the precipitation of the δ-phase.

Acknowledgements

Authors are thankful to Dr Placid Rodriguez, Director, Dr Baldev Raj, Director, Materials, Chemical and Reprocessing Groups, Indira Gandhi Centre for Atomic Research, Kalpakkam, for their keen interest in this work. The authors wish to acknowledge Mr A.L.E. Terrance, Scientific Officer, Physical Metallurgy Section, IGCAR, for his valuable discussions and Mrs C. Sudha for carrying out the EPMA analysis.

References

[1] H.L. Eiselstein, D.J. Tillack, in: E.A. Loria (Ed.), Superalloy 718, 625 and Various Derivatives, TMS, Warrendale, PA, 1991, p. 1.
[2] E.E. Brown, D.R. Muzyka, in: C.T. Sims, W.C. Hagel (Eds.), The Superalloys II, Wiley, New York, NY, 1987, p. 165.
[3] H. Bohm, K. Ehlrich, K.H. Krammer, Metallurgy 24 (1970) 643.
[4] F. Garzarotli, A. Gerscha, F.P. Francke, Z. Metallkd. 60 (1969) 643.
[5] S. Floreen, G.E. Fuchs, W.J. Yang, in: E.A. Loria (Ed.), Superalloys 718, 625, 706 and Various Derivatives, TMS, Warrendale, PA, 1994, p. 13.
[6] M. Sundararaman, P. Mukhopadhyay, S. Banerjee, Metall. Trans. A 19A (1988) 453.
[7] M. Sundararaman, P. Mukhopadhyay, S. Banerjee, Mater. Sci. Forum 3 (1985) 273.
[8] I. Kirman, J. Iron Steel Inst. 207 (1969) 1612.
[9] D.R. Muzyka, in: C.T. Sims, W.C. Hagel (Eds.), The Superalloys, Wiley, NewYork, 1972, p. 113.
[10] M. Sundararaman, L. Kumar, G.E. Prasad, P. Mukhopadhyay, S. Banerjee, Metall. Mater. Trans. A 30A (1999) 41.
[11] J.F. Radavich, A. Fort, in: E.A. Loria (Ed.), Superalloys 718, 625, 706 and Various Derivatives, TMS, Warrendale, PA, 1994, p. 635.
[12] C. Thomas, P. Tait, Int. J. Pressure Vessels Piping 59 (1994) 41.
[13] H.W. Tawancy, R.B. Herchenrocder, A.J. Asphanani, J. Met. 35 (1983) 37.
[14] H.W. Tawancy, Metall. Trans. A 11A (1980) 1764.
[15] B.K. Shah, P.P. Nanekar, M. Mukhopadhyay, A.K. Bandhopadhyay, A.K. Biswas, P.G. Kulkarni, in: 14th World Conference on Non-Destructive Testing (14th WCN DT), New Delhi, India, December 1996, p. 2235.
[16] G.E. Prasad, M.K. Asundi, Trans. IIM 42 (1989) 291.
[17] M. Kumar, V.K. Vasudevan, Acta Mater. 44 (1996) 1591.
[18] H.M. Tawancy, J. Mater. Sci. 16 (1981) 2883.